



Missouri University of Science and Technology
Scholars' Mine

International Conferences on Recent Advances
in Geotechnical Earthquake Engineering and
Soil Dynamics

1991 - Second International Conference on
Recent Advances in Geotechnical Earthquake
Engineering & Soil Dynamics

12 Mar 1991, 2:30 pm - 3:30 pm

Laboratory Tests on Embedded Reactor Building on Soft Ground

Itaru Kurosawa
Shimizu Corporation, Tokyo, Japan

Shohara Ryoichi
Shimizu Corporation, Tokyo, Japan

Kinji Akino
Nuclear Power Engineering Test Center, Tokyo, Japan

Masanori Izumi
Tohoku University, Japan

Follow this and additional works at: <https://scholarsmine.mst.edu/icrageesd>

 Part of the [Geotechnical Engineering Commons](#)

Recommended Citation

Kurosawa, Itaru; Ryoichi, Shohara; Akino, Kinji; and Izumi, Masanori, "Laboratory Tests on Embedded Reactor Building on Soft Ground" (1991). *International Conferences on Recent Advances in Geotechnical Earthquake Engineering and Soil Dynamics*. 10.

<https://scholarsmine.mst.edu/icrageesd/02icrageesd/session02/10>

This Article - Conference proceedings is brought to you for free and open access by Scholars' Mine. It has been accepted for inclusion in International Conferences on Recent Advances in Geotechnical Earthquake Engineering and Soil Dynamics by an authorized administrator of Scholars' Mine. This work is protected by U. S. Copyright Law. Unauthorized use including reproduction for redistribution requires the permission of the copyright holder. For more information, please contact scholarsmine@mst.edu.



Laboratory Tests on Embedded Reactor Building on Soft Ground

Itaru Kurosawa, Shohara Ryoichi
Nuclear Power Division, Shimizu Corporation, Tokyo, Japan

Kinji Akino
Nuclear Power Engineering Test Center, Tokyo, Japan

Masanori Izumi
Professor, Dept. of Architecture, Tohoku University, Japan

SYNOPSIS : Model tests using shaking table and impulse hammer were performed to confirm analysis tools currently used in Japan for the seismic design of a reactor building embedded in soft ground. The models are made of a silicone rubber ground and an aluminum building. Embedment depths of the foundation are varied. Comparison between test results and analytical results is discussed in terms of impedance functions, foundation input motions and structure responses.

INTRODUCTION

Analysis tools considering the effects of embedment on seismic response of buildings have become available in recent years. However, there are still lack of experimental research works. The purpose of this test is to experimentally confirm the seismic analysis tools used in Japan for the seismic design of a reactor building embedded in soft ground, where soil-structure interaction effect is predominant on the vibration characteristics of the building.

OUTLINE OF TESTS

Two series of testing were conducted. One is the series of ground-foundation interaction tests with varying embedment depths of the foundation (to a depth of 0cm, 9cm, 18cm). And the other is the series of ground-building interaction tests. To grasp the vibration characteristics of the ground model, the ground model was subjected to a shaking table test. In addition, a foundation was installed in the pit of the ground model and impulse hammering and shaking table tests were conducted.

Ground model

The ground model is a cylinder with a diameter of 3m and height of 70cm, and has a pit 18cm deep in the center.

The shape of the pit is a 40cm x 40cm square at bottom and a 76cm x 76cm square at the top surface level, and the side slope angle is 45°. The material is silicone rubber designed to have Young's modulus of 3 kg/cm² to simulate the soft ground taking into account the scale effect.

The sketch of the ground model is shown in Fig.1. In order to obtain the exact properties of the silicone rubber used for the ground model, the velocity of S wave and P wave in the ground model was measured.

The average travelling velocity was $V_p = 913$ m/s for P wave and $V_s = 10.76$ m/s for S wave. The

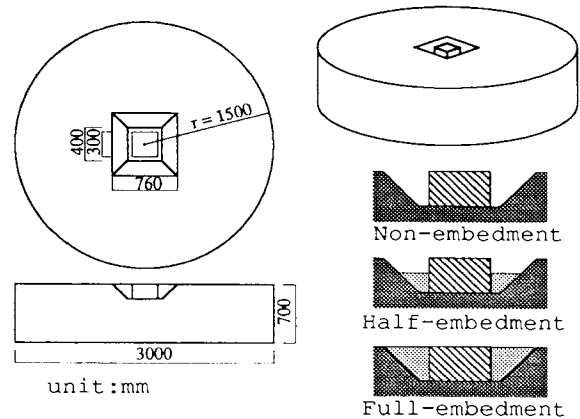


Fig.1 Ground and Foundation Models

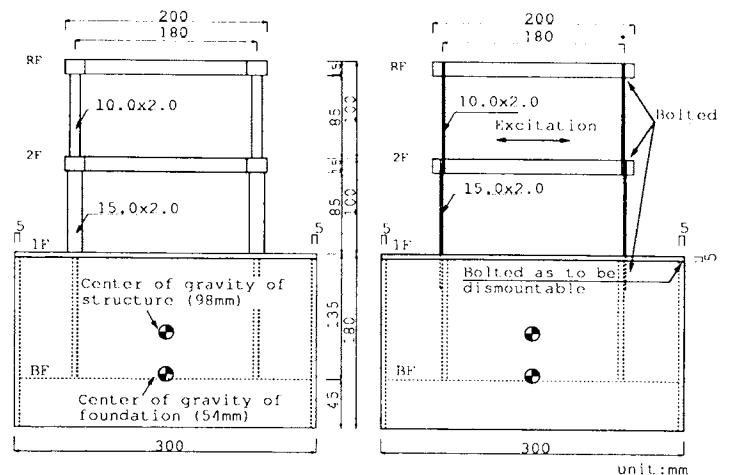


Fig.2 Reactor Building Model

calculated Poisson's ratio from the test results is $\nu = 0.49993$. Also, the shear elasticity modulus G is 1.18 kg/cm^2 and the Young's modulus E is 3.54 kg/cm^2 .

Building model

The Rigid foundation part to be embedded and floor of 2F and RF of the building model are composed of aluminum and the pillars are phosphor bronze spring material. Since the tests were carried out for the foundation alone and with the upper structure mounted, the foundation part and the upper structure are so bolted as to be dismountable.

The outline of the building model is shown in Fig. 2. Dimension of the building model is shown in Table. 1.

Hammering test

Hammering test was carried out to determine the vibration characteristics of the building model, and to evaluate the vibration characteristics of the ground-foundation interaction system and the ground-building interaction system. Excitation was applied with an impulse hammer equipped with a load cell contact at the tip.

In normal exciting by hammering, transfer function (acceleration/force) of the vibration system is usually derived, referring to "data processing by transient response (Mita A. et al.(1989))" to remove the reflected waves from the boundary in these tests, excitation force and wave shape of acceleration itself were recorded. At foundation exciting in the ground-foundation tests, the tests at different excitation positions were carried out, namely excitation was applied to the top of foundation (at 1cm above the bottom plate in the foundation), and at the top of the attachment.

Shaking table test

Shaking table tests were carried out applying seismic and sinusoidal waves. The shaking table has a size of $4\text{m} \times 4\text{m}$ and it is capable of six degrees of excitation.

(1) Sinusoidal excitation

Excitation steps were discontinuous with constant acceleration (20gal and 100gal), in which frequency was changed in steps. Excitation frequency range was 1~50Hz, with normal frequency intervals of 0.2Hz, and of 0.1Hz in the vicinity of the resonance frequency.

(2) Seismic excitation

Following the scale rule of the model, the time axis was multiplied by a factor of 1/3 and the duration time was set as 8.33 seconds. Figure 3 illustrates the time history of acceleration and its response spectrum of the earthquake used. The input to the shaking table was modified applying the transfer function determined through the ground model tests to reproduce the wave illustrated in Fig. 3 at the ground surface level.

Table.1 Dimensions of Building Model

Lumped masses	Mass1		
	Weight	(kg)	1.6
	Moment of inertia	($\text{kg} \cdot \text{cm}^2$)	53.6
	Mass2		
	Weight	(kg)	1.6
	Moment of inertia	($\text{kg} \cdot \text{cm}^2$)	53.6
Foundation	Weight	(kg)	16.0
	Moment of inertia	($\text{kg} \cdot \text{cm}^2$)	1790.0
	Height of gravity	(cm)	5.4
Columns	Height of gravity	(cm)	9.8
	Upper columns		
	Section	(mm)	10.0x2.0
	Horizontal stiffness	(t/m)	4.2
	Rotational stiffness	($\text{t} \cdot \text{m}/\text{rad}.$)	31.9
	Lower columns		
	section	(mm)	15.0x2.0
	Horizontal stiffness	(t/m)	6.3
	Rotational stiffness	($\text{t} \cdot \text{m}/\text{rad}.$)	39.1

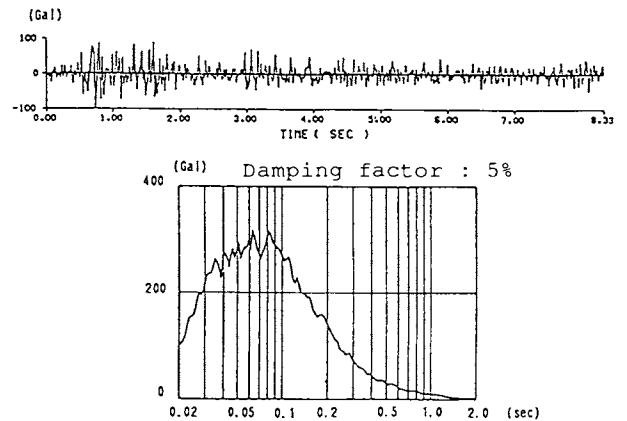


Fig.3 Time history of Acceleration and its Response Spectra of Seismic Excitation

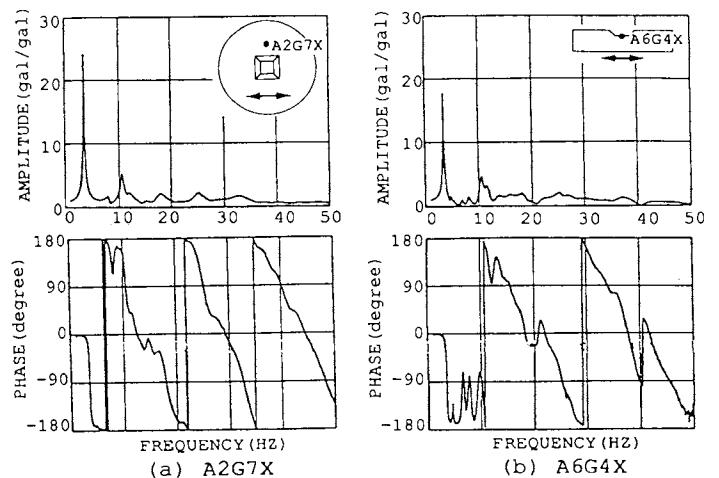


Fig.4 Acceleration Transfer Functions for Sinusoidal Shaking Table Test

TEST RESULTS

Ground Model Excitation Test

Figure 4 shows the acceleration transfer functions for the horizontal component when the ground model was excited in the horizontal direction. The transfer function is a ratio of the acceleration at every point on the ground model to the acceleration on the shaking table. Peaks were clearly observed near 3.5 Hz, 10 Hz, 17 Hz and 24 Hz, which are considered as corresponding to the first, second, third and fourth modes. At A2G7X, a slight disturbance took place in the frequency range between system frequencies. At the center (A6G4X) on the bottom of the pit, moreover, complex curves appeared, which could be supposed to arise under the influence of the pit.

Ground-foundation interaction test

(1) Hammering test

Figure 5 illustrates the difference of the transfer function by embedded depth in the exciting tests by the impulse hammer. Here the transfer function when the exciting is applied to the top of the attachment is shown. By the half embedding of the foundation part, peak amplitude decreases to 1/3, and by the full embedding, decreases to another 1/2. There is also delay of phase. The peak frequency also increases a little by increase of degree of embedding. These results display the increase of the rigidity and the damping of the system with increase of embedment depth.

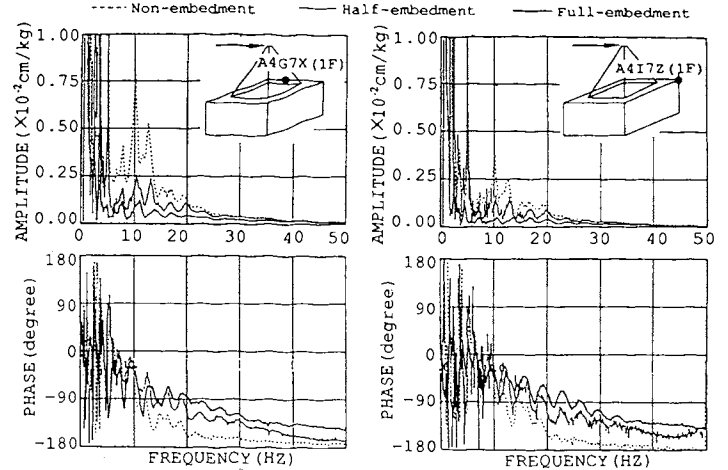
(2) Shaking table test

Figure 6 compares the transfer functions obtained by the shaking table tests with reference to embedment depth. As a reference point of transfer function, the average of five points at pit bottom in ground model tests is utilized. As in foundation exciting tests, by the half embedding on the side of the foundation, amplification ratio decreases to 1/2. By full embedding it still decreases as compared to the half embedded case. The position of $-\pi/2$ phase shifts to higher frequency a little by half embedding, but the full embedded case is not much different with the half embedded case.

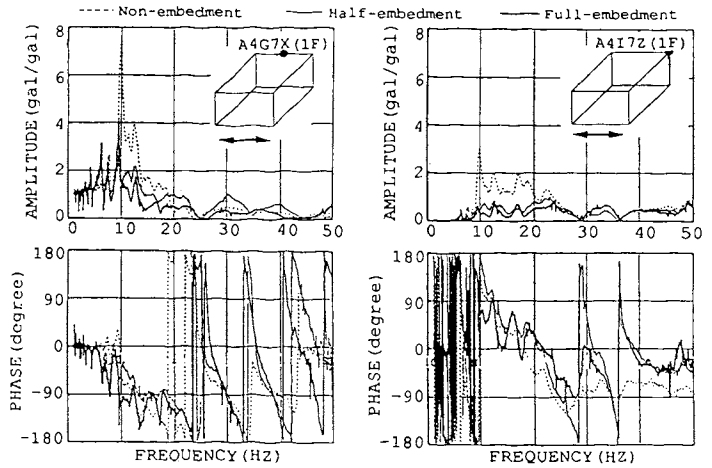
(3) Identified impedance functions

Since the ground has an S-wave velocity of 10.36 m/s., approximately 0.1 second ($=0.52 \times 2/10.36$) is required for the S-wave generated with the foundation excited to reach the foundation after being reflected by the steel table. In addition, approximately another 0.1 sec is required for the same wave to reach the foundation on the bottom surface after being reflected again by the steel table of the ground model. A transfer function, therefore, was obtained by the use of the wave-forms of the following three durations:

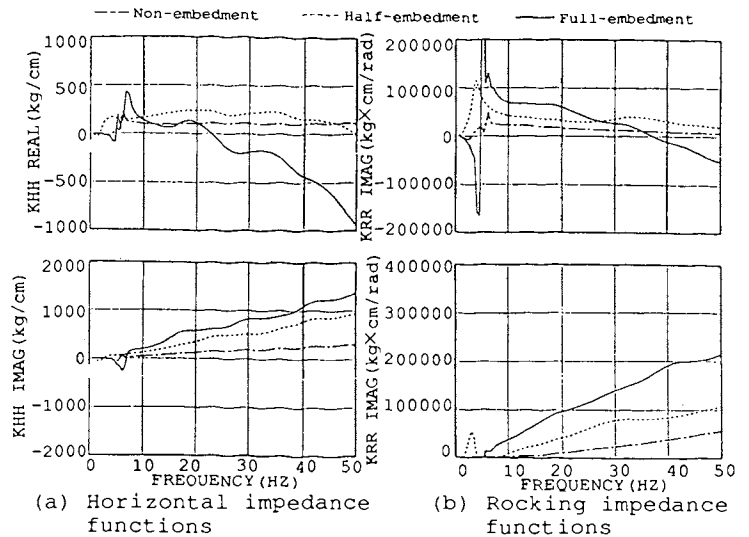
- (1) T = 0.1 (sec) : excluding all reflected waves
- (2) T = 0.2 (sec) : including the first reflected wave from the bottom
- (3) T = 2.0 (sec) : including all reflected waves



(a) Horizontal component (b) Vertical component
Fig.5 Displacement Transfer Functions for Hammering Test



(a) Horizontal component (b) Vertical component
Fig.6 Transfer Functions for Sinusoidal Shaking Table Test (20gal)



(a) Horizontal impedance functions (b) Rocking impedance functions
Fig.7 Impedance Functions (T=0.1sec)

The identified impedance functions were compared, and the effect of embedment on the identified impedance functions were studied in Fig. 7. The imaginary part tends to increase with increasing embedment depth. The real part, in the full embedded case, has a tendency of decreasing towards high frequency, and the order of magnitude of the impedance function of each embedment depth changes as the frequency changes. However, at 7.0Hz ~ 10.0Hz, the value of identified impedance function increases with embedment depth.

(4) Foundation input motions

Figure 8 illustrates foundation input motions. As a reference point of transfer functions, the average of five points at pit bottom in ground model tests is utilized. The horizontal component of the foundation input motion, in case of non embedded, has an amplitude of almost 1.0 and phase almost 0.0. However in the half embedded and full embedded cases, from 10.0Hz on the amplitude decreases and the phase is delayed. Rotational component exists in all cases, but is largest in the non embedded case. If there is no pit, there should arise no rotational component in the non embedded case, therefore it is apparent that the pit has a significant effect on the foundation input motion.

Ground-building interaction test

(1) Hammering test

The transfer functions from the vibration tests by hammering, are compared in Fig. 9. The amplitude decreases to 1/3 by change from non embedded to half embedded, and again to 1/2 by change to full embedded. If the frequency at which the phase is $-\pi/2$ can be considered as the primary system frequency, the system frequency increases and its amplitude decreases with increase of embedment depth. From these observations, it is evident that the stiffness and damping ratio increase with embedment depth.

(2) Shaking table test

Sinusoidal and seismic excitations were performed as described below. Figure 10 compares the transfer functions with different embedment depth, with the average of five positions in bottom of the pit as a reference. Though the change of primary system frequency and amplification property are visible in the hammering test, they are not in the shaking table test. Figure 11 compares the soil pressure transfer function of the foundation bottom and the foundation side with different embedment depth. In the foundation bottom soil pressure, half embedding depresses rocking vibration resulting in decrease of amplitude to less than 1/3. Full embedding, compared to half embedding, depresses it slightly more but the difference is small. As for the side soil pressure, at upper observation position (PP6E2X) up to 20Hz, half embedded displays higher values. The acceleration response spectra at seismic excitation in relation with embedment depth is shown in Fig. 12. The damping constant is set at 5%, and in order to realize constant exciting

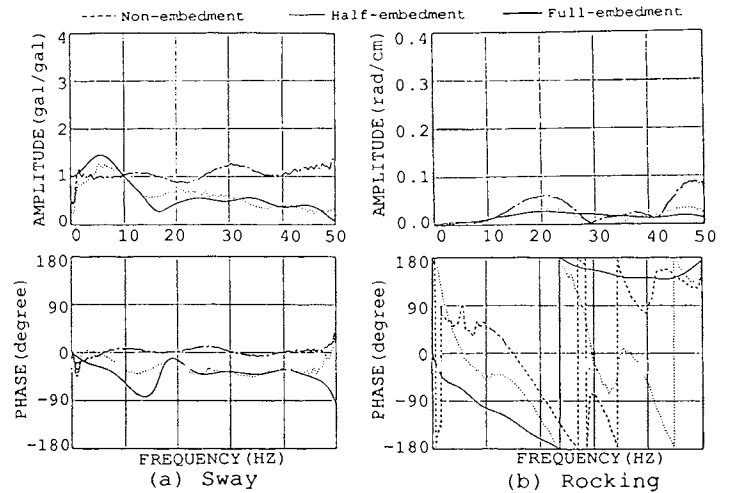


Fig.8 Foundation Input Motion (T=0.1sec)

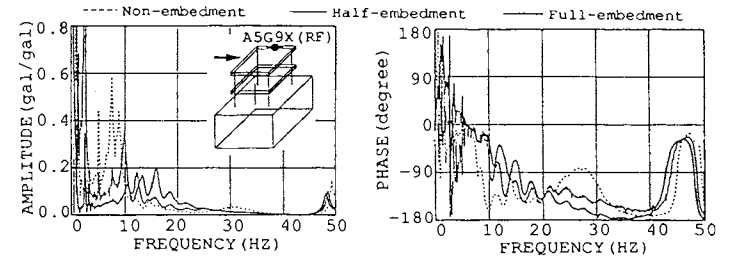


Fig.9 Displacement Transfer Functions for Hammering Test

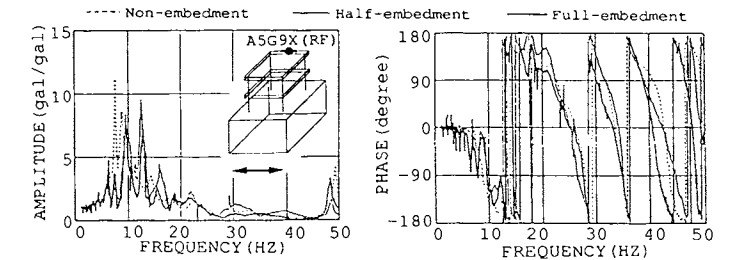


Fig.10 Transfer Functions for Sinusoidal Shaking Table Test (20gal)

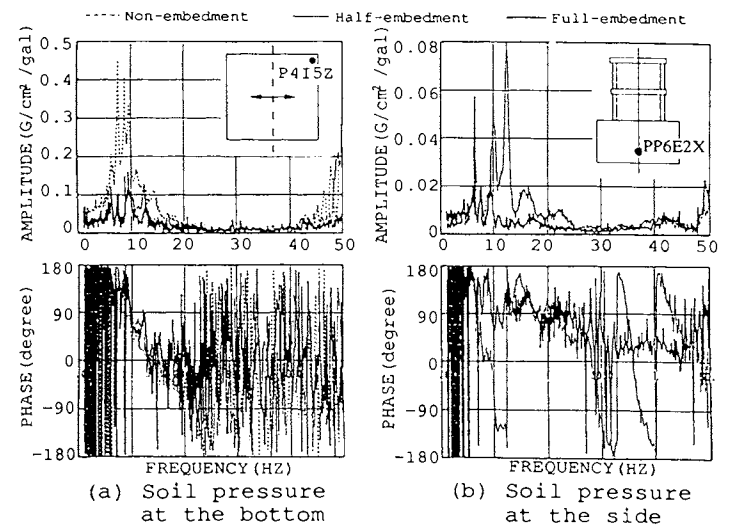


Fig.11 Transfer Functions of Soil Pressure for Sinusoidal Shaking Table Test (20gal)

level, maximum acceleration is normalized to be 300gal at ground level (A2G7X). Results at ground level (A2G7X) in all cases give similar spectrum patterns, indicating the similar excitation was applied in all tests. Spectra at building top decrease with increasing the embedment depth and the peak shifts toward higher frequency.

Figure 13 shows the distribution of maximum response acceleration of the model building. The maximum response value in the full embedded is smaller than in the half embedded. Response at the building top is larger in the half embedded than in the non embedded.

(3) Natural frequency and displacement mode ratio

The displacement mode ratio at the frequency where the transfer function phase comes to $-\pi/2$ first is shown in Table. 2. As the embedment depth increases, the frequency increases, and the ratio of elastic deformation of the upper structure tends to increase. As sway ratio of the half embedded and the full embedded are 6% and 0% respectively, height of rotation center is increased with increasing embedment depth.

ANALYSIS AND EVALUATION OF TEST RESULTS

Outline of analysis

The analytical investigation of the test results, in the non embedded and half embedded cases were carried out. Two analytical methods were used: (1) S-R Model employing the bottom surface spring obtained by the boundary element method and the side spring obtained by Novak et al.(1978), and (2) Axi-symmetric FEM. Since there is tendency to evaluate the stiffness higher than the actual value in an analysis by FEM, the material constant of the ground model was determined beforehand to simulate the ground model test results using axi-symmetric FEM.

In the S-R model, however, since there is little possibility of evaluating the rigidity higher than the actual value, material constants obtained by the material test results were used as obtained, except for Poisson's ratio.

S-R Model Analysis

(1) Analysis conditions

The S-R model for the half embedment was used. The impedance function is defined at the center of the foundation bottom surface. This impedance function was compared with the test result. The impedance function obtained from the boundary element method was used as the impedance function of the bottom surface. Novak's spring on uniform ground was used as the impedance function on the side of a portion to be embedded, because both the support ground and the backfill had been set to an identical level of rigidity.

Figure 14 shows the concept of the analysis model and the ground constants applied to the analysis.

(2) Comparison with test results

Figure 15 is a comparison of test results for the non embedded foundation test results with the

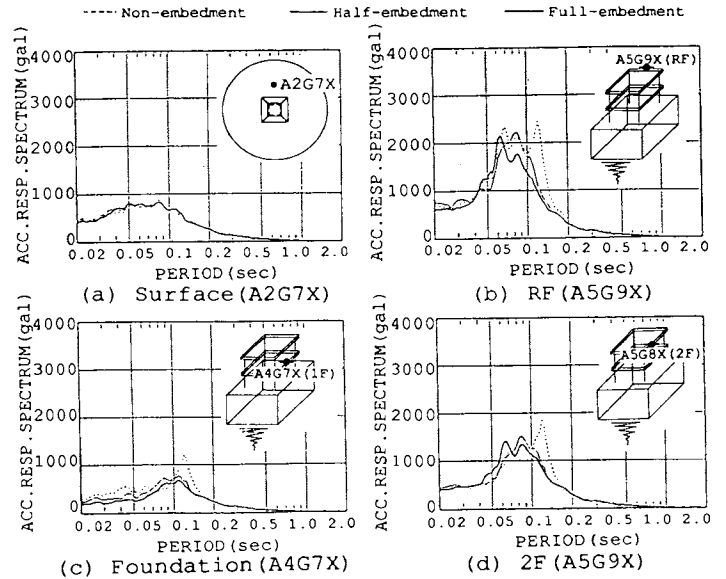


Fig.12 Acceleration Response Spectra for Seismic Excitation Test

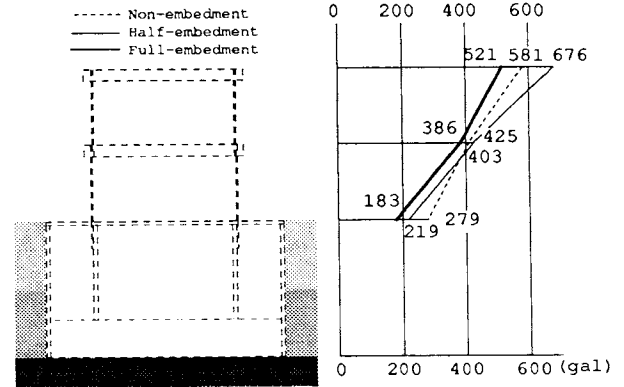


Fig.13 Maximum Acceleration for Seismic Excitation Test

Table.2 Displacement Mode Ratio at the Top of Test Model

Test	Embedment	Frequency* (Hz)	Sway (%)	Rocking (%)	Elastic Deformation (%)
Ground Model + Building Model	Non-Embedment	8.1	20	52	28
	Half-Embedment	10.1	6	60	34
	Full-Embedment	13.5	0	20	80

*Frequency when the Phase Reaches $-\pi/2$ for the First time

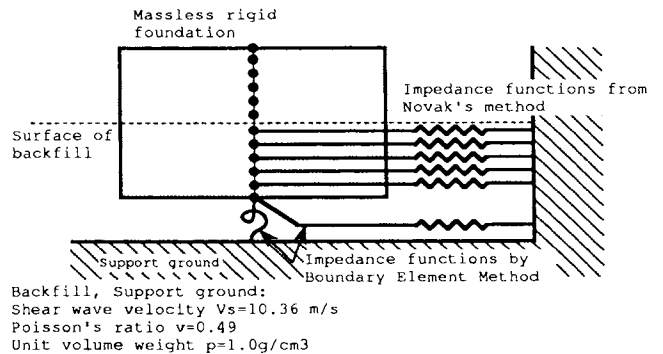


Fig.14 Concept of the S-R Model and Material Constants Applied to the Analysis

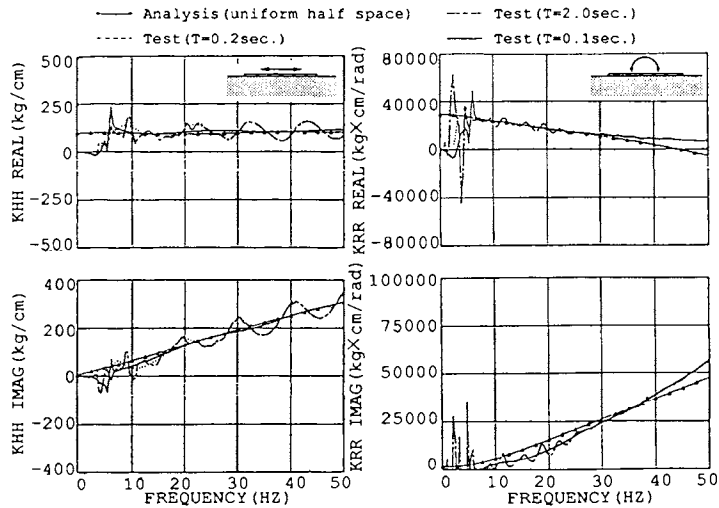
bottom spring obtained by the boundary element method. The analysis value for a uniform half-space agreed well with the test value with a duration of 0.1 sec assumed. The test values with duration times of 0.2 and 2.0 sec oscillate around the test value of the duration time 0.1 sec. Figure 16 compares test results for the half embedded foundation with analysis values. Those analysis values are the sum at the center of the foundation on the bottom surface, with Novak's side spring added. Unlike the test value, the real horizontal impedance function decrease from 10 Hz and turn to negative from 25 Hz. The reason of this derivation is due to the value of the Poisson's ratio of the soil material which close to 0.5 and Novak's equation reaches to non-applicable range.

Axi-symmetric FEM Analysis

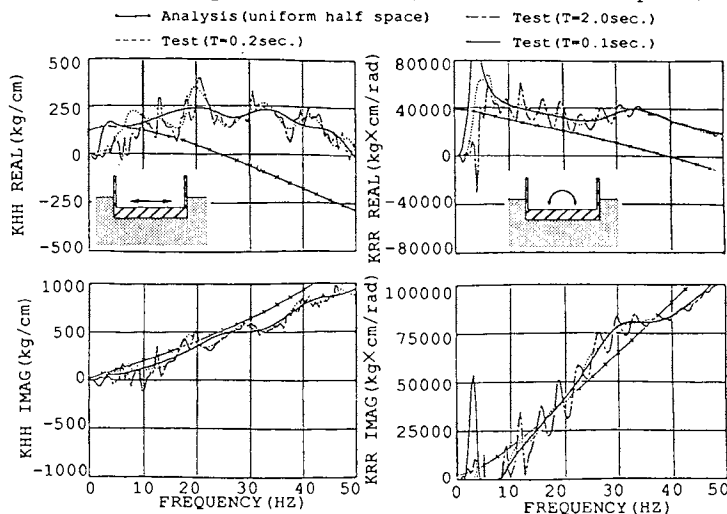
The axi-symmetric FEM model of the foundation half-embedded in an uniform half space is shown in Fig. 17. At the side transmitting boundary and at the base viscous boundary are assumed. The shape of the foundation is a square parallelepiped but here it is substituted by a circular cylinder. The impedance functions obtained by the axi-symmetric FEM in the non embedded case are compared with the identified impedance functions obtained by corresponding tests in Fig. 18. Similar to the analysis by the boundary element method, the analysis values and the test values agree well. The identified impedance functions of the half embedded foundation in an uniform half space is shown in Fig. 19. Except for the amplitude of the horizontal impedance function, the agreement with the test value is better than the analysis value obtained by the S-R model. However, for the horizontal component, the test value is higher than analysis value at above 10.0Hz region. Since there is little difference between the analysis results by S-R model where the pit can not be taken into consideration, and the analysis results by axi-symmetric FEM, where the pit is considered, the effect of the pit on the impedance functions can be regarded to be small.

(1) Foundation input motion

Analysis results of foundation input motion based on data within 0.1 seconds of excitation which simulate the uniform half space were compared and studied. The analysis was carried out by using axi-symmetric FEM for the uniform half space. The horizontal component of foundation input motion in the non embedded case is compared in Fig.20(a) and the rotational component is compared in Fig. 20(b). The horizontal component is in good agreement for both amplitude and phase, but for rotational component, in frequency of above 10Hz, there is some difference between values obtained by the tests and those obtained by the analysis. This might be due to modelling of the rectangular pit by an axi-symmetric cylinder. The horizontal component of the foundation input motion of half embedded case is shown in Fig. 21(a) and the rotational component in Fig. 21(b). In the half embedded case, the correspondence of rotational component of test values and analysis values are better than in



(a) Horizontal impedance functions (b) Rocking impedance functions
Fig.15 Comparison of Impedance Functions for Non-Embedded Foundation Between Test and Analysis(S-R Model, Uniform Half-space)



(a) Horizontal impedance functions (b) Rocking impedance functions
Fig.16 Comparison of Impedance Functions for Half-embedded Foundations Between Test and Analysis(S-R Model, Uniform Half-space)

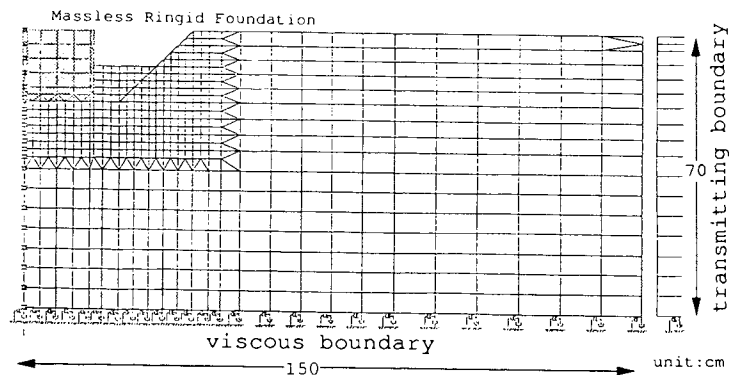


Fig.17 Model for axi-symmetric FEM (Ground + Foundation, Half-embedment, Uniform half-space)

the non embedded case. This is due to the decrease of pit shape effect on the foundation input motion by the half embedding. As described above, different from the case of impedance function, the effect of pit on the foundation input motion is prominent.

(2) Transfer function

(i) Transfer function of building for hammering test

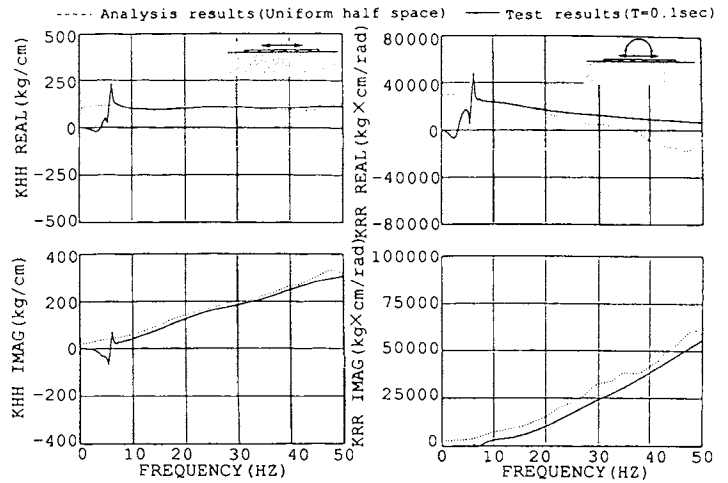
Figure 22(a) compares the test values and the analysis values by an axi-symmetric FEM in the non embedded case. Around the primary system frequency, the analysis values are in good agreement with the test values both for amplitude and phase. Figure 22(b) compares the test values and the analysis values of transfer function in the half embedded case. Around the primary system frequency, the analysis values of frequency are slightly higher compared to the test values.

(ii) Transfer function of building for shaking table test

The transfer function of the building by the shaking table test in the non embedded case is shown in Fig. 23(a). For the reference point of transfer function, the average of five positions at pit bottom in ground model tests is utilized. In the transfer function of RF, the amplitude at around 15Hz is larger in the analysis values than in the test values. As described above, shape of the pit of ground model is rectangular in the tests, but is replaced by a circular circular in the analysis. This results in larger foundation input motions, especially its rotational component in the analysis values compared with the test values. The transfer function in the half embedded case is the shown in Fig. 23(b). Difference observed in the non embedded case around 15Hz decreases, which implies the decrease of effect of the pit as its depth decreases.

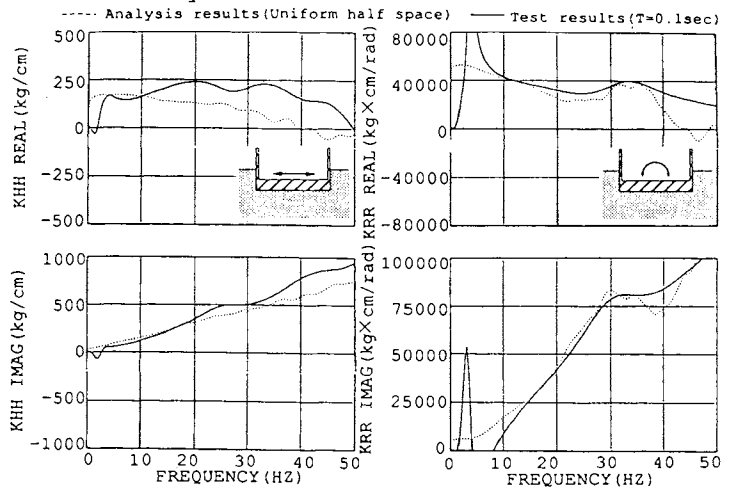
CONCLUSION

Two series of testing were conducted. One was a series of ground-foundation interaction tests with the varied embedment depths of the foundation from non embedded to full embedded. And the other was a series of ground-building interaction tests. The results of these tests have been studied and summarized as follows:
 (a) As a result of testing the ground-foundation interaction system, it was confirmed that embedding the foundation decreases the amplitude of the transfer function while the radiation damping increases.
 (b) As a result of testing the ground-building interaction system, it was verified that embedding decreases the amplitude of the transfer function and that the primary system frequency increases.
 (c) For the displacement mode ratio in the ground-foundation interaction test, embedding suppressed rocking while promoting sway. and increased the elastic deformation ratio.
 (d) The imaginary parts of the impedance function identified from the test results increased due to the embedding. However, the order of the



(a) Horizontal impedance functions (b) Rocking impedance functions

Fig.18 Impedance functions for Half-embedded Foundation (Uniform half-space Axi-symmetric FEM)



(a) Horizontal impedance functions (b) Rocking impedance functions

Fig.19 Impedance functions for Half-embedded Foundation (Uniform half-space Axi-symmetric FEM)

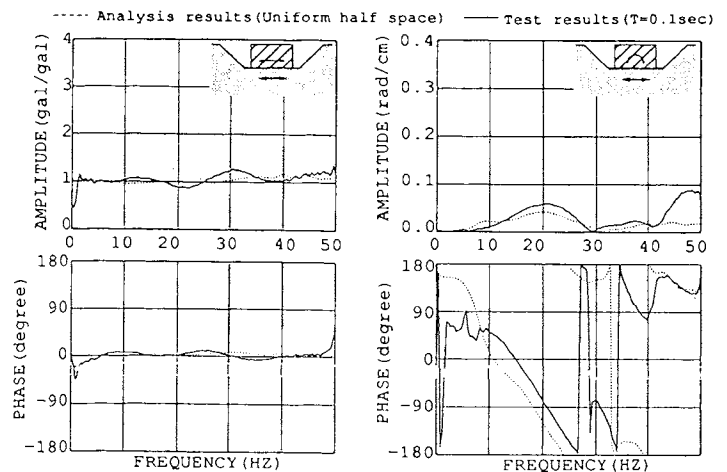


Fig.20 Foundation Input Motion for Non-embedded Foundation (Uniform half-space Axi-symmetric FEM)

magnitude of the real part of the impedance function of each embedment depth changes as the frequency changes.

(e) Complex frequency characteristics are shown in both the impedance function and the foundation input motion, which were obtained from the transfer function under the steady response containing the boundary effects of the ground model. Nevertheless, both the identified impedance function and foundation input motion are available in a smooth shape through data processing by the use of transient responses. Good coincidence was found in relation to the axi-symmetric FEM analysis which simulates a uniform half space.

(f) The impedance function obtained by the S-R model with the Novak spring employed on the side showed tendency different from that of the test value.

ACKNOWLEDGEMENTS

This work was carried out as the entrusted project sponsored by the Ministry of International Trade and Industry in Japan. This work was supported by "Sub-Committee of Embedment Effect on Reactor Building" under "committee of Seismic Verification Tests" of NUPEC. The authors wish to express their gratitude for the cooperation and valuable suggestion given by the members of Committee.

REFERENCES

Izumi, M. et al., "Model Tests on Embedment Effect on Reactor Building - Laboratory Test (part 1-4)", Summaries of Technical Papers of Annual Meeting Architectural institute of Japan, 1989, vol.C, pp.1079-1086. (In Japanese)

Izumi, M. et al., "Model Tests on Embedment Effect on Reactor Building - Laboratory Test (part 5-7)", Summaries of Technical Papers of Annual Meeting Architectural institute of Japan, 1990, vol.C, (submitting). (In Japanese)

Izumi, M. et al., "Study on the Effect of Pit on Soil-Structure Interaction (Part1,2)", Summaries of Technical Papers of Annual Meeting Architectural institute of Japan, 1990, vol.C, (submitting). (In Japanese)

Novak, M. et al. (1978) "Dynamic Soil Reactions for Plane Strain Case" EM4, ASCE.

Mita, A. et al. (1989), "Soil-Structure Interaction Experiment Using Impulse Response" EESD., Vol.18

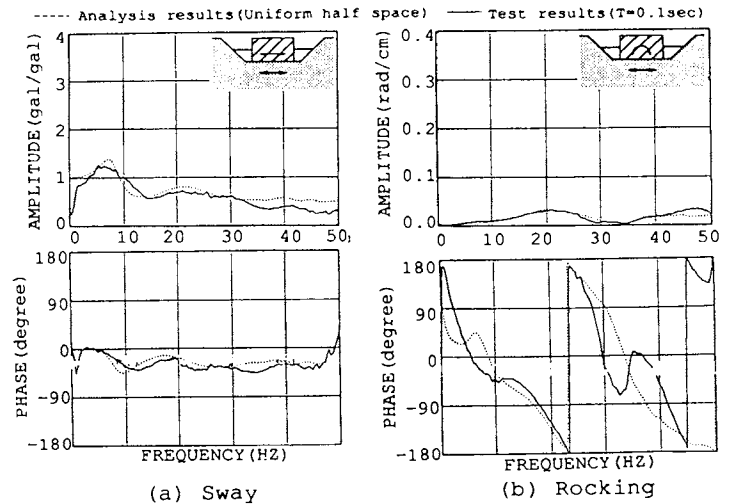


Fig.21 Foundation Input Motion for Semi-embedded Foundation (Uniform half-space, Axi-symmetric FEM)

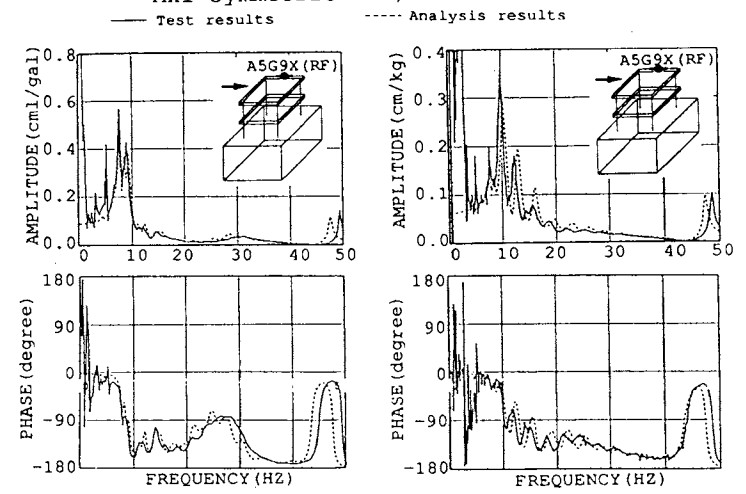


Fig.22 Transfer Functions of the Building for Hammering Test (Finite ground, Axi-symmetric FEM)

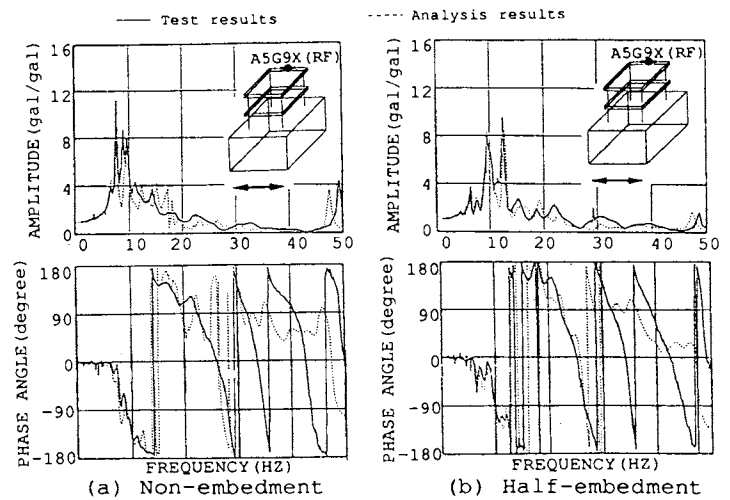


Fig.23 Transfer Functions of the Building for Shaking Table Test (Finite ground, Axi-symmetric FEM)